Electronic properties of beryllides of the rare earth and some actinides

E. Bucher,* J. P. Maita, G. W. Hull, R. C. Fulton, and A. S. Cooper
Bell Laboratories, Murray Hill, New Jersey 07974
(Received 14 March 1974)

A magnetic study has been conducted of 17 beryllides of the form $M\mathrm{Be}_{13}$, M being a rare earth, Th, U, and an alloy $\mathrm{La}_{0.75}\mathrm{Tm}_{0.25}$. Specific-heat studies were also made for M = La, Pr, Sm, Tm, Lu, Th, and U. A thorough crystal-field analysis is presented for PrBe_{13}, TmBe_{13}, both ions being in a crystal-field singlet ground state, and the expected nuclear cooling and ordering behavior is also thoroughly discussed.

I. INTRODUCTION

Beryllium is known to form numerous compounds with almost all elements of the Periodic Table. The few systematic studies among several structure groups showed a very interesting behavior, especially the Be-rich compounds $X\mathrm{Be}_{22}$ (X= Mo, W, Tc, Re) exhibiting high superconducting transition temperatures, although maintaining the basic properties of pure Be of extremely low electronic specific heat and high Debye temperatures.[1] $\mathrm{Be}_{12}\mathrm{Cr}$, on the other hand, was recently found to belong to the class of itinerant ferromagnets.[2] $M\mathrm{Be}_{13}$ is another example of Be-rich compounds. M may stand for any alkali-earth element, a rare earth including Sc, Y, or an actinide element as well as some of the early 4d and 5d transition elements.[3] These compounds belong to the cubic NaZn_{13} structure-type family[4] which can be considered roughly as a CsCl-type structure, consisting of a Zn_{13} (Be_{13}) complex as one giant ligand and Na(M). The M-M separation is in all cases 5 Å or more.[5] In the case of the actinide compounds this leads to well-localized 5f states.[6] Furthermore, the electronic properties are expected to be predominantly due to the majority component, as was similarly demonstrated previously for the $X\mathrm{Be}_{22}$ series.[1]

In this paper we will confine our discussion to the $M\mathrm{Be}_{13}$ series with M being a rare earth, Th and U. These compounds have the advantage of being the only intermediate phase between Be and the rare earth, Th and U.[7] The main interest will concentrate on the magnetic and crystal-field properties and some applications thereof, such as nuclear cooling and nuclear ordering. In order to derive crystal-field splittings from the Schottky specific heat the electronic and lattice part had to be measured independently from a nonmagnetic "background" material, such as LaBe_{13}, LuBe_{13}, or ThBe_{13}. Therefore, we will also discuss some of their thermal properties, all the more as our results are in strong conflict with some of the results recently published after completion of this work.[8]

In Sec. II, we will describe the preparation procedures and some metallurgical aspects of the materials and also the experimental equipment. In Sec. III, we will discuss the properties of the compounds, one by one, and summarize all the results in Table I.

II. EXPERIMENTAL PART

A. Sample preparation

One of the major problems in handling Be and its compounds is their known toxicity,[9] in particular, as far as volatile dust is concerned. This is the major reason why extremely little work has been done on these otherwise interesting compounds. If handled carefully, solid Be compounds are no more dangerous than any other toxic elements such as Tl, Hg, Pb, Cd, As, Se, Te, etc.

A study of the $M\mathrm{Be}_{13}$ phases[7] shows melting points considerably higher than the individual components, reflecting the high stability of these compounds, in turn reflected by their congruent melting behavior. Very often this means a strong reduction of the partial vapor pressures of one or even both components. As a matter of fact, this was at least qualitatively observed during the fusion of EuBe_{13}, SmBe_{13}, YbBe_{13}, or TmBe_{13}, where both components have prohibitively high vapor pressures at the melting point of ~1900 °C. We took advantage of this fact when reacting the two components. Reaction starts immediately at the melting point of the lower melting component. The higher melting component is immediately dissolved to form the compound. If thus reacted carefully, weight losses of Be are almost negligible. Some difficulties occurred in the cases of EuBe_{13} and YbBe_{13}, where the rare-earth loss was considerable at the first reaction and which had to be compensated at least twice. Borsa and Olcese[8] prepared their samples by solid-state reaction, which is highly inadequate and presumably the main reason for our discrepancy with their results.

For magnetic measurements, samples of approximately 10–20 mg total weight were reacted in

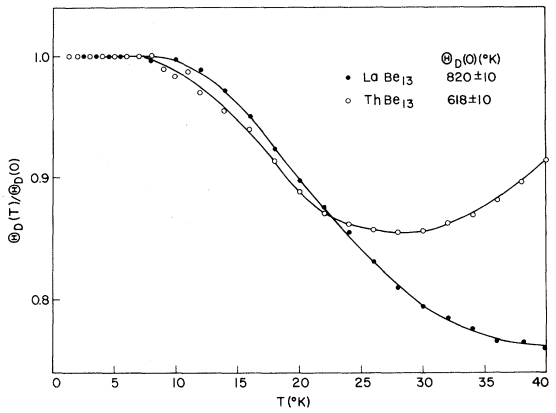

FIG. 1. Reduced Debye temperature $\Theta_D(T)/\Theta_D(0)$ for $LaBe_{13}$ and $ThBe_{13}$.

an argon arc furnace. For specific-heat measurements, semispheres of 0.5–0.8 g of $LaBe_{13}$, $PrBe_{13}$, $SmBe_{13}$, $TmBe_{13}$, $LuBe_{13}$, $ThBe_{13}$, and UBe_{13} were melted. All MBe_{13} phases show a brilliant silvery color. The compounds are extremely brittle and show large crystallites with easy cleavage planes. All the compounds investigated are very stable in air. Except for UBe_{13}, the samples were measured in the as-cast state. After completion of the melting process, the argon arc furnace was sealed off from the pumping line and opened up behind a protected hood. The whole arc furnace was flooded with very dilute acid and water flushed several times in order to avoid any possible contamination from Be. Be was purchased as 99.99% pure distilled lumps (United Mineral and Chemical Corp., New York) and the rare earths were nominally 99.9% pure (Lunex and Research Chemicals, USA), Th and U were 99.99% and 99.96% pure crystal bar material.

The specific heat was measured in a heat-pulse calorimeter between 1.4 and 45 °K.[10] Among the magnetic compounds, only $PrBe_{13}$, $SmBe_{13}$, $TmBe_{13}$, and UBe_{13} were measured. The magnetic contribution of $PrBe_{13}$, $TmBe_{13}$, and UBe_{13} was separated by subtraction of the specific heat of $LaBe_{13}$, $LuBe_{13}$, and $ThBe_{13}$, respectively. For the interpretation of $SmBe_{13}$, the lattice and electronic part is negligible up to 20 °K. Susceptibility was measured in a pendulum magnetometer[11] between 400 and 1.3 °K in fields between 1.2 and 15 kOe. Low-field susceptibilities were also measured by an ac mutual-induction method (1.3 Oe, 25 Hz) between 50 and 0.45 °K. Owing to the large ratio of surface tension/density, the small magnetic samples were almost ideal spheres for which a well-defined demagnetization factor of $n=\frac{1}{3}$ could be applied.

After completion of all the measurements, the samples were broken in a sealed plastic bag and small chips picked out for x-ray measurements in a Gandolfi camera. The lattice constants obtained from these measurements are in most cases in good agreement with previously published values.[7]

III. RESULTS AND DISCUSSION

All the results are summarized in Table I. Some recent experimental data from Borsa and Olcese[8] and Domngang and Herr[12] differ strongly from our data. We feel it convenient to discuss the materials in groups related to the same physical problems.

A. $LaBe_{13}$, $LuBe_{13}$, $ThBe_{13}$

These three nonmagnetic compounds were investigated mainly to isolate the magnetic data of isomorphous magnetic compounds. We note that these compounds show properties characteristic of pure (hcp) Be.[13] $LaBe_{13}$ and $LuBe_{13}$ are diamagnetic and have very low electronic specific heats and high Debye temperatures. The latter two properties are ideal for an accurate analysis of the Schottky specific heat up to relatively high temperatures (30–40 °K). $LaBe_{13}$ and $LuBe_{13}$ served to subtract the lattice and electronic specific heat from $PrBe_{13}$ and $TmBe_{13}$, respectively, in order to derive the crystal-field properties of the latter from their Schottky anomaly. The properties of $ThBe_{13}$ are very similar to $LaBe_{13}$ and $LuBe_{13}$, and the valence difference is not strongly reflected in the electronic properties. The electronic specific heats are very close to the values of the superconducting XBe_{22} series, although the nonmagnetic MBe_{13} phases do not show superconductivity down to 0.45 °K. The insertion of a heavy mass such as La, Lu, Th, into a light Be matrix might lead to an expected low-frequency Einstein mode. Instead $\Theta_D(0)$ drops approximately by a factor of 2. $\Theta(T)/\Theta(0)$ is shown in Fig. 1 and does not support the idea of a localized Einstein mode. The susceptibility of all three compounds is extremely weak and therefore no background correction was necessary in any of the magnetic compounds. We would like to point out however, that our weak diamagnetism for $LaBe_{13}$ of -24×10^{-6} cm^3/mole (1 mole corresponds here to the weight of a formula unit) differs from the value of $+190\times10^{-6}$ cm^3/mole given by Borsa and Olcese.[8]

B. $CeBe_{13}$, $YbBe_{13}$

Both compounds have anomalously low and high lattice constants, respectively, indicating some intermediate valence state. $CeBe_{13}$ was previously discussed by Cooper *et al.*[14] and Borsa and Olcese.[8] Qualitatively we find the same behavior of $CeBe_{13}$ with a flat susceptibility maximum near 140 K; however, our values of χ_m are over 20% lower over the whole temperature range.

TABLE I. Lattice constants, Néel-temperature, susceptibilities, paramagnetic ordering temperatures, and effective moments for MBe_{13} compounds.

Compound	Lattice[a] constant (Å)	T_N (°K)	χ (cm^3/mole)[a]	Θ_p (°K)	P_{eff}	Other properties[e]
$LaBe_{13}$	10.451		-24.10^{-6} [b]			$\gamma = 0.58$ mJ/°K^2 g atom, $\Theta(0) = 820$ °K, not superconducting above 0.45 °K
$CeBe_{13}$	10.372		1.64×10^{-3} [b]	complex		χ_{max} near 140 °K $= 1.92\times10^{-3}$ cm^3/mole
$PrBe_{13}$	10.369		0.0470[c]	−8	3.58	$A_4\langle r^4\rangle = +2.85$ meV $x = -0.70$ $A_6\langle r^6\rangle = +0.70$ meV $W = 2.08$ °K
$NdBe_{13}$	10.348	2.63		+2.5	3.57	
$SmBe_{13}$	10.304	8.8				λ-type specific-heat anomaly at 9.05 °K $(C/R)_{max} = 3.6$
$EuBe_{13}$	10.286		6.47×10^{-3} [c]			
$GdBe_{13}$	10.273	25.7		+25	7.94	
$TbBe_{13}$	10.247	15.3		14.0	9.71	
$DyBe_{13}$	10.233	9.3		13	10.47	
$HoBe_{13}$	10.219	5.45		+6	10.57	
$ErBe_{13}$	10.203	2.37		+6	9.53	
$TmBe_{13}$	10.189		2.59[c]	+1	7.55	$A_4\langle r^4\rangle = -0.412$ meV $x = 0.35$ $A_6\langle r^6\rangle = +0.177$ meV $W = -0.134$ °K
$YbBe_{13}$	10.180		1.25×10^{-3} [b] 3.2×10^{-3} [d]			
$LuBe_{13}$	10.170		-125×10^{-6} [b]			not superconducting above 0.45 °K $\gamma = 0.60$ mJ/°K^2 g atom, $\Theta_D = (930 \pm 20)$° K
$La_{0.75}Tm_{0.25}Be_{13}$	10.394		2.31[c]		7.56	χ flat below 0.9 °K
$ThBe_{13}$	10.383		$(16 \pm 3)\times10^{-6}$ [b]			not superconducting above 0.45 °K $\gamma = 0.507$ mJ/°K^2 g atom $\Theta_D(0) = 618$ °K, $d\chi/dT \sim 0$
UBe_{13}	10.257			−98	3.52	no ordering down to 0.65 °K

[a] This work.
[b] At 300 °K.
[c] At 1.0 °K.
[d] At 77 °K.
[e] χ is defined for 1 mole of rare earth except in $La_{0.75}Tm_{0.25}Be_{13}$ where it is taken for 1 mole of Tm^{3+}.

$YbBe_{13}$ also shows complex magnetic behavior with an intermediate valence state. It exhibits a value of $\chi_m(300\ °K) = 1.25\times10^{-3}$ cm^3/mole, increasing to 3.2×10^{-3} cm^3/mole Yb at 77 K, with non-Curie-Weiss behavior down to He temperatures.[15]

C. $EuBe_{13}$, $PrBe_{13}$, $TmBe_{13}$, UBe_{13}

The first three compounds in this group have a nonmagnetic singlet ground state and do not show magnetic order down to 0.45 °K. UBe_{13} does not show magnetic order down to 0.65 °K and we consider the singlet only as the most probable ground state, by analogy with $PrBe_{13}$.

D. $EuBe_{13}$

This is one of the rather rare intermetallic compounds in which Eu is in the 3+ state leading to an orbital singlet $J = 0$. The next higher multiplet $J = 1$ is expected to lie at approximately $\Delta = 41.1_4$ meV (Ref. 16) above the $J = 0$ ground state. This leads to a theoretical Van Vleck susceptibility $\chi(T = 0)$ of 6.29×10^{-3} cm^3/(mole Eu) given by

$$\chi(0) = 8N\mu_B^2/\Delta \ . \qquad (1)$$

Our value of 6.47×10^{-3} cm^3/mole is ~3% higher, which may be due to weak exchange effects and/or slight off-stochiometry of the sample.

As we will show later, the point symmetry of Eu in $EuBe_{13}$ is cubic; and there is no crystal-field splitting of the $J = 1$ state. Therefore, an analysis of the Van Vleck susceptibility may serve to determine the spin-orbit coupling constant Δ. Neglecting for the moment the uncertainty in stochiometry of $EuBe_{13}$, we may introduce a small exchange cor-

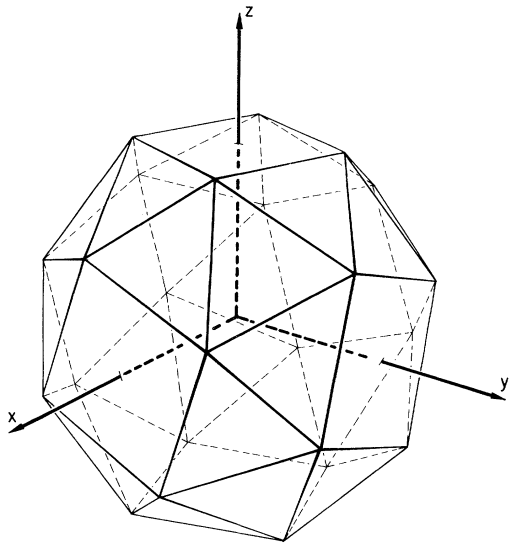

FIG. 2. Nearest-neighbor Be polyhedron (snub cube) in the $M\mathrm{Be}_{13}$ compounds. M is at (0, 0, 0) and the snub cube is assumed to be regular. The system of fourfold axis was chosen to derive the first-neighbor crystal-field potentials given by expressions (4) and (5).

rection which may conveniently be taken from $\Theta_p = 24.5\ ^\circ\mathrm{K}$ (paramagnetic Curie temperature) of GdBe_{13}, which we assume to have an exchange character identical with EuBe_{13}. From the molecular-field equation

$$\chi = \chi_0/(1 - \lambda\chi_0)\ , \tag{2}$$

where χ_0 is given by (1) and $\lambda = \Theta_p/C$ of GdBe_{13}, where C is the Gd Curie constant, we find $\chi_0 = 6.34 \times 10^{-3}$ cm^3/mole, with our χ value given in Table I. Analyzing other Eu^{3+} compounds with cubic point symmetry (such as $EuPd_3$, $EuRb_2NaF_6$, etc.) we find an average χ_0 value of $6.31 \times 10^{-3} \pm 0.03 \times 10^{-3}$ cm^3/mole close to the value of EuBe_{13}. From our average χ_0 we find a spin-orbit coupling constant Δ of 41.0 ± 0.3 meV, in excellent agreement with Gardner *et al.*'s value of 41.1_4 meV.[16] This consistency, obtained from several different materials including intermetallic compounds and insulators, leads to the conclusion that Δ is indeed a purely intra-atomic property and if affected at all by the chemical bond, these effects must be extremely small, probably less than 0.5%.

E. Structural considerations

In order to understand crystal-field behavior we present some basic features of the NaZn_{13} structure type, discussed by Shoemaker *et al.*[4] The cubic unit cell contains eight formula units. The M ions have eight equivalent positions at $\pm(\frac{1}{4}, \frac{1}{4}, \frac{1}{4})$, whereas Be has two inequivalent positions, namely 8 $\mathrm{Be_I}$ in (0, 0, 0), $(\frac{1}{2}, \frac{1}{2}, \frac{1}{2})$ and 96 $\mathrm{Be_{II}}$ at $\pm(0, y, z)$; $\pm(0, y, \bar{z})$; $\pm(\frac{1}{2}, z, y)$; $\pm(\frac{1}{2}, \bar{z}, y)$, plus threefold rotation and face-centering equivalent positions. The M-$\mathrm{Be_I}$ system thus forms a simple CsCl-type lattice with a lattice constant $\frac{1}{2}$ of $M\mathrm{Be}_{13}$. $\mathrm{Be_I}$ is surrounded by a $\mathrm{Be_{II}}$ icosahedron (coordination $z = 12$), whereas M is surrounded by 24 $\mathrm{Be_{II}}$ sitting at the corner of a snub cube (coordination $z = 24$). There is no set of parameters (y, z) for which both the icosahedron and the snub cube are regular. The regularity condition of the snub cube requires $y = 0.1761$, $z = 0.1141$.[4] Baenziger and Rundle[17] and Gladyshevskii *et al.*[18] found values of 0.178 and 0.112, respectively, for CeBe_{13}. The deviation from regularity is therefore small and will not affect the crystal-field calculations. In Fig. 2, we show the polyhedron formed of the 24 nearest $\mathrm{Be_{II}}$ neighbors. It consists of 32 regular triangles and six squares, depicting the four-fold axis which we chose as coordinate axis. It leads to the usual crystal-field Hamiltonian

$$\mathcal{H}_{CF} = B_4(O_4^0 + 5O_4^4) + B_6(O_6^0 - 21O_6^4)\ , \tag{3}$$

given by Lea-Leask-Wolf[19] (LLW) for simpler coordination. After some lengthy calculation we find in the first-neighbor point-charge approximation using LLW notation:

$$B_4 = -0.12022_8(Z_1e^2/R_1^5)\langle r^4\rangle\beta\ , \tag{4}$$

$$B_6 = -0.02183_4(Z_1e^2/R_1^7)\langle r^6\rangle\gamma\ . \tag{5}$$

The second neighbors of M are eight $\mathrm{Be_I}$ neighbors in primitive cubic point symmetry, at a distance $R_2 \approx 1.470R_1$ [R_2 would be $1.490R_1$ for the y, z parameters analyzed by Shoemaker *et al.* for NaZn_{13} (Ref. 4)]. The 24 $\mathrm{Be_{II}}$ third neighbors are at $R_3 \times 1.503\ R_1$ and another 24 $\mathrm{Be_{II}}$ fourth neighbors at $R_4 = 1.523\ R_1$. These distances were calculated using properties of the regular icosahedron and snub cube and maybe as much as 2% off for other than our y, z values used. It must be emphasized that the (unscreened) B_4 contribution of the second neighbors is not small (~48%) compared to B_4 due to the first neighbors, but it is strongly cancelled by higher neighbors and since we do not know the amount of electronic shielding we make the rough assumption to neglect all higher neighbor's crystal-field contribution. It should also be kept in mind that the crystal-field contribution due to second and third neighbors cannot be written in the simple form of (3) because the cubic axis of these higher neighbors do not coincide with the ones shown for the first neighbors in Fig. 2. With these facts and restrictions in mind we can now proceed to calculate effective point charges from derived crystal-field potentials.

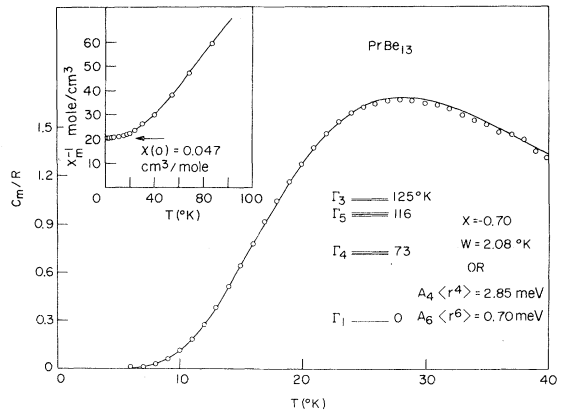

FIG. 3. Schottky anomaly C_m/R, crystal-field levels, and inverse low-temperature susceptibility vs temperature of $PrBe_{13}$.

F. $PrBe_{13}$

Preliminary data on this compound have been published previously.[20,21] The $^3H_4$ state shows a relatively large crystal-field splitting with a Γ_1 crystal-field ground state.

In Fig. 3 we show the Schottky specific heat of $PrBe_{13}$ along with the inverse susceptibility versus temperature. We have made use of LLW who give the relative splitting of the crystal-field levels vs x, defined as

$$B_4F(4) = Wx\,, \tag{6}$$

$$B_6F(6) = W(1 - |x|)\,, \tag{7}$$

where W is an energy-scaling parameter and $F(4)$ and $F(6)$ are numerical constants given in Ref. 19. The Schottky anomaly was calculated for $-1 \le x \le 1$ in steps of 0.05 and 0.01, where necessary for a normalized overall splitting of 1. The parameter x and W giving the best fit were then chosen and $A_4\langle r^4\rangle = B_4/\beta$ and $A_6\langle r^6\rangle = B_6/\gamma$ calculated. All numbers are shown in Table I. The analysis of the Schottky anomaly turned out to be ambiguous over the temperature range measured. The second set of parameters x, W near $x = -0.15$, yields a crystal-field susceptibility of 0.031 cm^3/mole compared to 0.044 cm^3/mole for our chosen parameters. This compares much better with our experimental value of 0.047 cm^3/mole. As we can see from other ordering compounds or from $EuBe_{13}$, exchange effects are very weak and could not account for such a large shift in crystal-field susceptibility. From $A_4\langle r^4\rangle$ we calculate $Z_1 = +1.9_8|e|$, using $\langle r^4\rangle$ of Freeman and Watson.[22] This number would be reduced to $+1.2_2|e|$ using relativistic values of $\langle r^4\rangle$.[23] The corresponding numbers Z_1 from $A_6\langle r^6\rangle$ are $+16.0|e|$ and $+7.8|e|$, respectively. As usual, the effective point-charge model is violated, yielding sixth-order crystal-field potentials far too low compared to experimental values. However, both crystal-field potentials lead to a positive-ligand-charge model.[21]

We shall postpone the discussion of nuclear and hyperfine properties of $PrBe_{13}$ until we have discussed $TmBe_{13}$ and instead consider the $5f$ analog of $PrBe_{13}$, namely UBe_{13}.

G. UBe_{13}

This compound has been measured previously by Troć *et al.*[6] It was concluded that U has a rather well-localized $5f^2$ configuration, and thus it is the $5f$ analog to $PrBe_{13}$. One might therefore expect a similar crystal-field pattern with a singlet Γ_1 lowest. Owing to the more spread-out $5f$ wave function, the overall splitting is expected to be considerably larger than in $PrBe_{13}$. However, neither in the measurements of Troć *et al.*,[6] nor in our own measurements of various samples made from different U lots with different heat treatments, was it possible to observe a temperature-independent Van Vleck susceptibility at low temperature. We tried to detect any possible magnetic ordering below 1 °K. Instead we found a sharp superconducting transition at 0.97 °K, which was reduced by about 0.3 °K only in a field of 60 kOe. This suggests that the superconductivity is not an intrinsic property of UBe_{13}, but probably linked with precipitated filaments. Subsequent powdering did not shift nor reduce the superconducting signal, although calibration with a Pb cylinder showed that the signal of UBe_{13} was only about 50% of the expected full signal. From the fact that none of the other MBe_{13} phases showed superconductivity down to 0.45 °K, one is tempted to conclude that the superconductivity and perhaps also the susceptibility tail at low temperature is due to precipitated U filaments. Various samples made with excess or Be deficiency led to the same results. X-ray analysis yielded the single phase lines of UBe_{13} only, which, according to the well-established phase diagram, is the only existing intermetallic compound, even with congruent melting behavior.[7] Specific-heat measurements between 1.8 and 42 °K, shown in Fig. 4, remained likewise inconclusive. At low temperature there is no exponential behavior. Instead there is a large low-temperature tail with an upturn starting below 4 °K. Unfortunately, in spite of our serious effort we have no clear answer to offer about the nature of UBe_{13}.

H. $TmBe_{13}$

The magnetic specific heat versus temperature of this compound is shown in Fig. 5, magnetization curves at 1.49 and 4.30 °K and low temperature

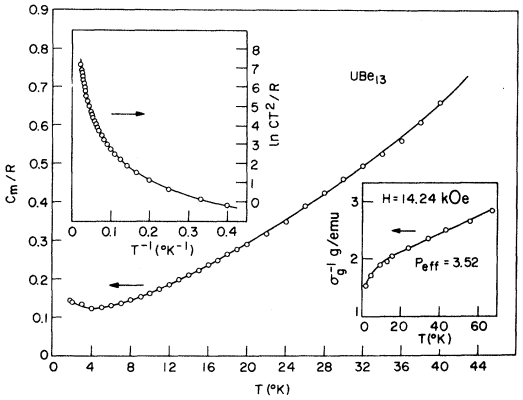

FIG. 4. Magnetic specific heat C_m/R, inverse magnetization per gram vs temperature, and $\ln(C_mT^2/R)$ vs inverse of temperature for UBe_{13}.

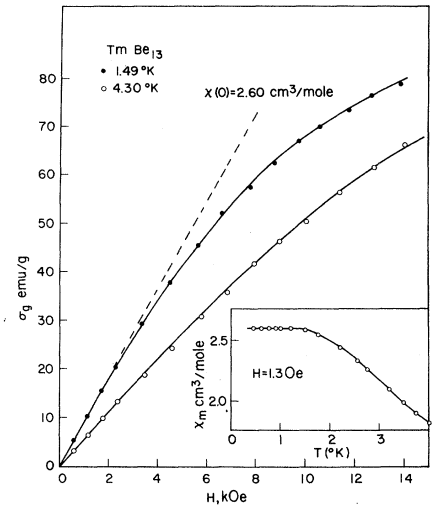

FIG. 6. Magnetization curves of $TmBe_{13}$ at 1.49 and 4.30 K and low-field low-temperature susceptibility vs temperature.

susceptibility are shown in Fig. 6. For the analysis of the Schottky specific heat, we followed the same procedure described under $PrBe_{13}$, leading to the level system indicated in Fig. 5. Experimentally the Schottky anomaly can be determined rather accurately over a wide temperature range, due to a relatively small overall splitting and extremely small electronic and lattice specific-heat corrections. At 15 °K these corrections amount to about 8%, increasing rapidly with increasing temperature.

From the relative level splitting given by LLW it was not possible to obtain a perfect fit over the whole temperature range. One may think of various reasons for this: (a) slight deviations from the LLW diagrams due to some irregularities of the nearest neighbor polyhedron, (b) exchange effects, which are not small,[24] and (c) spin-phonon interaction,[25] all of which in principle could distort a Schottky anomaly somewhat. Therefore, some uncertainty is inherent in our given level sequence of Fig. 5, in spite of the experimental accuracy. However, the ground state is Γ_2, regardless of the temperature range over which one tries to obtain the best fit. Our theoretical solid curve has to be considered as the best overall fit using the LLW model. Furthermore, we can make an entropy test of our measurement. Experimentally we find

$$\frac{1}{R}\int_{1.5°}^{15°}\frac{C_m}{T}dT = 2.254\,.$$

The values for S at 1.5 °K and

$$\frac{1}{R}\int_{15°}^{\infty}\frac{C_m}{T}dT$$

were calculated using the exact expression for S for the given set of levels in Fig. 5 and amount to 0.077 and 0.202, respectively. The latter value is identical to an experimental value obtained from a simple $1/T^2$ law of the high-temperature tail of the Schottky anomaly. The sum yields 2.533, compared to a theoretical value of $\ln 13 = 2.565$ ($J=6$ for Tm^{3+}). The experimental cutoff at 15 °K seems arbitrary, but was chosen because of some uncertainty of the Schottky anomaly above that temperature. This entropy test, together with our value of the effective moment very close to the theoretical value of the free ion, provides us with confidence in the quality of the MBe_{13} compounds, all prepared in the same way.

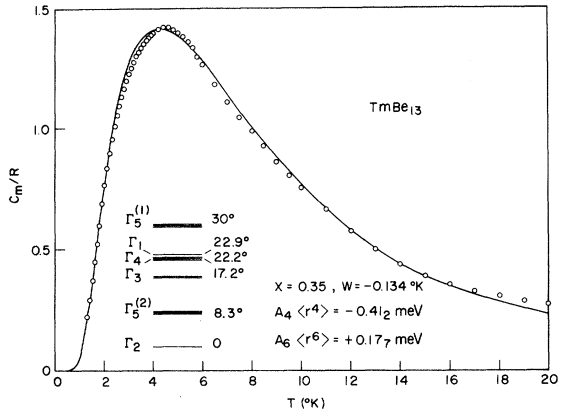

FIG. 5. Schottky specific heat of $TmBe_{13}$ and derived crystal-field levels.

The level sequence derived from the Schottky anomaly shows that the crystal-field ground state in $TmBe_{13}$ is also a singlet, but Γ_2 rather than Γ_1 as one would expect from similar parameters of $PrBe_{13}$. Surprisingly, we find even a change in

sign of $A_4\langle r^4\rangle$ as compared to $PrBe_{13}$. Formally, we can again derive Z_1 from $A_4\langle r^4\rangle$ and find $-0.69|e|$ and $-0.48|e|$ for nonrelativistic and relativistic $\langle r^4\rangle$ values, whereas $Z_1 = +15.4|e|$ and $+7.8|e|$ obtained from $A_6\langle r^6\rangle$ is practically the same as the one derived from $A_6\langle r^6\rangle$ of $PrBe_{13}$. The puzzling question, therefore, is why $A_4\langle r^4\rangle$ changes so strongly whereas $A_6\langle r^6\rangle$ remains almost unchanged. Such discrepancies in very dilute alloys of rare earths in various hosts have been explained recently[26] by the crystal-field contribution of virtually bound d electrons, giving a contribution to $A_4\langle r^4\rangle$ only. Intuitively one might expect a relatively larger $5d$ electron contribution in $TmBe_{13}$ than in $PrBe_{13}$ due to the $4f$ contraction, but this effect is very difficult to predict quantitatively.

From measurements presented in Figs. 5 and 6 we cannot exclude a possible magnetic phase transition occurring below 1 °K, therefore it was necessary to measure low-field susceptibility to below 1 °K. The susceptibility measured in a field of 1.3 G levels off below 1.5 °K with a temperature-independent value of 2.60 cm^3/mole, yielding also the correct low-field slope of the magnetization curve at 1.49 °K shown in Fig. 6. The pure-crystal-field susceptibility calculated from the level system of Fig. 5 would be only 1.72 cm^3/mole. A dilute compound $La_{0.75}Tm_{0.25}Be_{13}$ served roughly to test a molecular-field model for the exchange enhancement of the Van Vleck susceptibility. Its Van Vleck susceptibility is expected to be 2.10 cm^3/mole Tm^{3+}, as compared to the experimental value of 2.31 cm^3/mole Tm^{3+}. As observed previously,[27] the molecular-field theory is a rather poor approximation for such exchange enhanced materials. It should be noted that our Van Vleck susceptibility in $TmBe_{13}$ represents the highest value ever observed for intermetallic compounds, and exchange enhancement is quite appreciable (~ 50%). This has some interesting implications as far as nuclear adiabatic cooling and cooperative nuclear ordering is concerned.

I. Hyperfine properties of $TmBe_{13}$ and $PrBe_{13}$

Nuclear adiabatic demagnetization in Van Vleck paramagnets was first proposed by Al'tshuler[28] and has recently been experimentally demonstrated in numerous compounds.[29] An even more interesting observation was that the rare-earth nuclear system may undergo a cooperative magnetic order at temperatures up to ~ 50 mK.[30] The efficiency of this method is due to a strong enhancement effect of an externally applied magnetic field H_0 at the nuclear site given by

$$H_{hf}/H_0 = 1 + a\chi(0)/g_J\mu_B g_N\mu_N \ . \tag{8}$$

H_{hf} is the total hyperfine field seen by the nucleus, a is the hyperfine constant, the other symbols have their usual meaning. Previously determined numbers for H_{hf}/H_0 were between 4 and 100. Using Bleaney's[31] hyperfine constants, we calculate 9.74 and 452 for $PrBe_{13}$ and $TmBe_{13}$, respectively. The latter number is the largest ever calculated for all Van Vleck paramagnets explored thus far. It should be kept in mind that this number is only valid in the limit $H_0 \to 0$. Nuclear demagnetization of polycrystalline materials with such large enhancement factors, therefore, is problematic due to induced anisotropic strain, often causing nonisentropic behavior. Since our sample consisted of visibly large polycrystals, it was not meaningful to calculate the magnetization curve or even to try a nuclear demagnetization run. Nulcear demagnetization of various Van Vleck paramagnets, such as PrBi,[32] $PrTl_3$,[33] etc., showed a breakdown of the nuclear cooling which was demonstrated to be due to cooperative nuclear ordering of the rare-earth nuclei. The coupling mechanism invoked was an exchange coupling between the hyperfine induced $4f$ moments ΔJ, due to the presence of the nuclear spin I. ΔJ can simply be calculated from the hyperfine constants a and the tensor components $\chi_i(0)$ of the Van Vleck susceptibility:

$$\Delta J_i = \frac{a\chi_i(0)}{(g_J\mu_B)^2} I_i \ . \tag{9}$$

The exchange coupling can be evaluated using the electronic ordering temperature T_e of a neighboring compound with a certain J_{eff} in the crystal-field Kramers ground state. We then can write in molecular-field approximation

$$\frac{T_n}{T_e} \approx \frac{(g_J - 1)^2}{(g_{J'} - 1)^2}\left(\frac{\Delta J}{J_{eff}}\right)^2 \ . \tag{10}$$

In earlier cases,[29] (10) yielded nuclear ordering temperatures within a factor of 2 of experimentally observed values and we would like to evaluate at least the order of magnitude. We use $NdBe_{13}$ and $ErBe_{13}$ to evaluate T_n of $PrBe_{13}$ and $TmBe_{13}$, respectively. T_e is obtained from our Table I, whereas J_{eff} was taken from the wave functions given by LLW[19] obtained by interpolation of $A_4\langle r^4\rangle$ and $A_6\langle r^6\rangle$ between $PrBe_{13}$ and $TmBe_{13}$, using Freeman-Watson[22] values for $\langle r^4\rangle$. For $NdBe_{13}$ and $ErBe_{13}$ we find $J_{eff} = 2.09$ and 2.83, respectively. The results would be the same if $A_4\langle r^4\rangle$ and $A_6\langle r^6\rangle$ would be extrapolated from $PrBe_{13}$ to $NdBe_{13}$ and from $TmBe_{13}$ to $ErBe_{13}$. From (9) and (10) we calculate for the nuclear ordering temperature T_n of $PrBe_{13}$ and $TmBe_{13}$ ~ 0.2 and ~ 1.1 mK.

We believe that $PrBe_{13}$, in particular, would be an excellent candidate for the generation of submillidegree temperatures. This compound could also serve to cool He^3 down to well below 1 m °K for a possible search of superfluidity at zero pres-

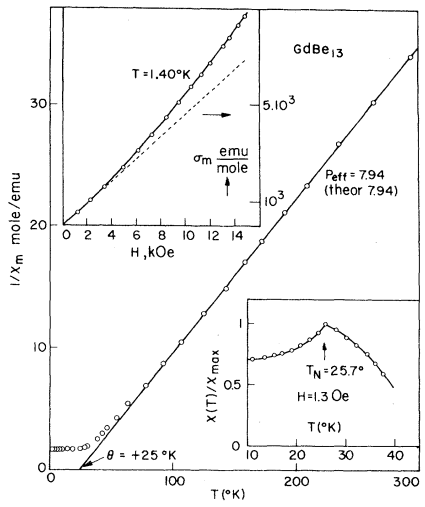

FIG. 7. $GdBe_{13}$: Inverse molar susceptibility in 14.24 kOe and relative low-temperature, low-field susceptibility vs temperature. Magnetization curve at 1.40 K.

sure. The possibility of magnetic surface states in Van Vleck paramagnets as suggested by Peschel and Fulde[34] could also be of considerable interest to break the Kapitza resistance to an experimentally acceptable order of magnitude.

For the remainder of the paper we will turn our attention to the magnetically ordering compounds, starting with the simplest one, $GdBe_{13}$, where no crystal-field effects are present.

J. $GdBe_{13}$

The most striking feature is the antiferromagnetic order, whereas from high-temperature extrapolation one would expect a ferromagnetic phase transition, due to $\Theta_p > 0$. We find $|T_N| \sim \Theta_p$ throughout the whole ordering series, even in those systems with crystal-field levels, except $ErBe_{13}$. In Fig. 7 we show the inverse susceptibility versus temperature T. In 14.24 kOe, no maximum in χ_m could be detected and the curve looks like a Van Vleck paramagnet. In the insert, χ_m vs T is shown in low fields, revealing the Néel temperature of 25.7 °K, and also a magnetization curve is given at 1.3 °K and up to 15 kOe. This behavior indicates that the magnetic order is probably of very complex nature.

In contrast to $GdBe_{13}$, most of the other ordering compounds in a non-S ground state show a much more pronounced structure in the magnetization curve at $T < T_N$. We ascribe this behavior to the crystal-field levels. If crystal-field splittings are relatively small, a field can have various effects resulting in additional admixture (besides the exchange field) of higher states Γ_i into the crystal-field ground state Γ_0, given by $\langle \Gamma_0 | J_z | \Gamma_i \rangle^2$. A second possibility is the Zeeman level crossing of adjacent crystal-field levels in high fields resulting in a step-like jump in the magnetization curve.[35] All these effects are strongly anisotropic, in particular if the Γ_8 quartets of Kramers ions are involved. Superposed on all these possibilities there is of course the nonlinearity in the magnetization curve due to the field-dependent spin-wave dispersion. All these effects generate a relatively complex magnetization curve, for which $DyBe_{13}$ (see Fig. 9 below) is perhaps the most striking example. Unfortunately, our coarse-grained polycrystals do not allow any further analysis of magnetization curves.

K. $SmBe_{13}$

We expect a Γ_8 quartet at ~12.5 °K above a Γ_7 ground state from an interpolation procedure. The specific heat in zero magnetic field shows a λ-type sharp peak at $T_N = 9.05$ °K, with a maximum $C/R = 3.6$, but no latent heat was detectable. $(1/R) \times \int_0^\infty (C_m/T)\, dT$ was determined and found to be 1.69, close to ln6 ($J = \frac{5}{2}$ for Sm^{3+}). No crystal-field splitting was detectable above T_N, which means that it is probably of the order of T_N. A flat shoulder occurs in the specific-heat curve at $T = 5.5$ °K and $C/R \sim 0.8$, which might be due to $\Gamma_7 - \Gamma_8$ splitting. The exchange splitting, however, makes a quantitative analysis difficult. Unfortunately our specific heat measurement is not conclusive enough to distinguish clearly between a Γ_7 or Γ_8 groundstate, although the shape of the specific-heat curve and the size of its anomaly would slightly favor a Γ_7 groundstate, i.e., a positive ligand charge model. At the lowest temperature we found the spin-wave specific heat to vary ~ $T^{2.8}$ and the magnetization curve was nearly linear from 0–15 kOe.

L. $TbBe_{13}$

The exact level sequence cannot be predicted here. Interpolation yields $x = -0.49$, with Γ_1 lowest. This is an x area where a lot of levels intersect. However, the crystal-field ground state is most probably a singlet, either Γ_1 or Γ_2 even if the Pr or Tm extreme values are taken for $A_4\langle r^4 \rangle$. Therefore, $TbBe_{13}$ is an induced-moment system, however, in the limit $T_N/\Delta \gg 1$ as the overall splitting W_0 is ~8 °K. The important quantity for an exchange-induced-moment system, the $\Gamma_1 - \Gamma_4$ or $\Gamma_2 - \Gamma_5^{(2)}$ splitting is almost an order of magnitude smaller than W_0. This can also be seen if Θ_p and T_N are plotted vs $(g_J - 1)^2 J(J+1)$. There is no detectable reduction for $TbBe_{13}$ which would be due to crystal-field splitting. On the other hand, $TbBe_{13}$ shows the strongest nonlinear magnetization curve (see Fig. 8) at $T \ll T_N$ which again we ascribe to the very small crystal-field splitting.

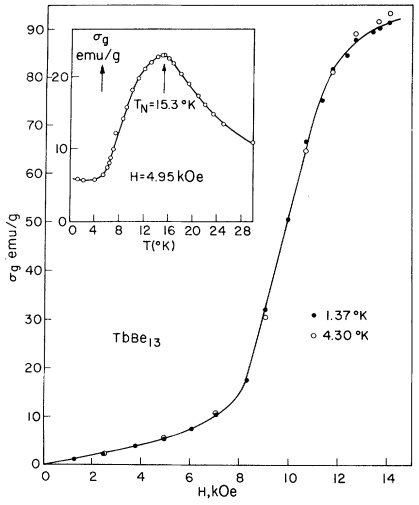

FIG. 8. Low temperature magnetization and susceptibility of $TbBe_{13}$.

M. $DyBe_{13}$

The level sequence in $DyBe_{13}$ is the same as in $ErBe_{13}$: Γ_7-$\Gamma_8^{(1)}$-Γ_6-$\Gamma_8^{(2)}$-$\Gamma_8^{(3)}$ and quite insensitive to errors in B_4/B_6 in the area $x=-0.07$. The overall splitting W_0 is only about 24 °K, again generating a rather complex magnetization pattern (see Fig. 9), as among five levels we have nine off-diagonal matrix elements different from zero.

N. $HoBe_{13}$

The crystal-field ground state is expected to be $\Gamma_3^{(2)}$, followed by $\Gamma_4^{(2)}$, irrespective of any interpolation procedure. Interpolation yields $x\sim-0.05$ and $W_0\sim 35$ °K and a $\Gamma_3^{(2)}$-$\Gamma_4^{(2)}$ splitting of only ~ 0.5 °K. Again, $HoBe_{13}$ has to be considered as an induced-moment system, however, with a non-Kramers (nonmagnetic) doublet as ground state. The splitting, however, is too small to generate Van Vleck paramagnetism and the exchange forces dominate strongly. Similar to $TbBe_{13}$, we are in the regime $T_N/\Delta \gg 1$, which is very little different from a magnetic groundstate (Δ is here the splitting between the lowest two levels) and the same nonlinear magnetization is observed as in other ordering compounds (Fig. 10).

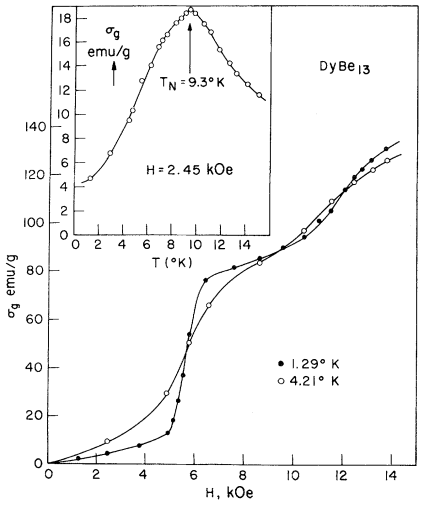

FIG. 9. Low temperature magnetization and susceptibility of $DyBe_{13}$.

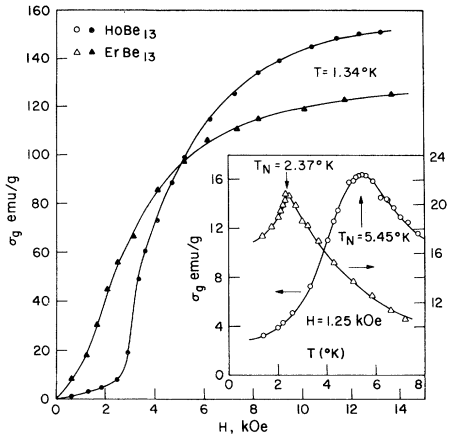

FIG. 10. Low-temperature magnetization and susceptibility of $HoBe_{13}$ and $ErBe_{13}$.

O. $ErBe_{13}$

The level sequence is Γ_7-$\Gamma_8^{(1)}$-Γ_6-$\Gamma_8^{(2)}$-$\Gamma_8^{(3)}$, the same as in $DyBe_{13}$, however, with an overall splitting of 35–40 °K. The larger splitting and weaker exchange field leads to a simpler magnetization curve at low temperature, compared to $DyBe_{13}$.

IV. CONCLUSIONS

The MBe_{13} series show the general features of other Be-rich lattices: low electronic specific heats and high Debye temperatures. These two properties are very favorable for studying the magnetic part of the specific heat of magnetic MBe_{13}.

For M=Eu, Pr, Tm we find Van Vleck paramagnetic behavior, whereas M=Ce, Yb show complex magnetic behavior due to an intermediate valence state. All other rare-earth compounds show magnetic order with a complex behavior: antiferromagnetic transitions with $\Theta_p>0$ and complex-magnetization curves for all ions with orbital momentum. UBe_{13} also has a complex behavior without a magnetic phase transition down to 0.65 °K or a

well-defined crystal-field splitting, although the effective moment corresponds accurately to U^{4+}.

$PrBe_{13}$ is suggested as a valuable candidate to generate very low temperatures well below 1 mK by hyperfine-enhanced nuclear adiabatic cooling. $TmBe_{13}$, on the other hand, has the largest hyperfine enhancement factor measured so far (452) and is expected to exhibit spontaneous nuclear ordering in the low-mK region.

ACKNOWLEDGMENTS

We are very grateful to Dr. R. J. Birgeneau and Professor B. Luthi for many critical and helpful comments on our work.

*Present address: University of Constance, Fachbereich Physik, P.O. Box 7733, D-775 Konstanz, Federal Republic of Germany.

[1]E. Bucher and C. Palmy, Phys. Lett. A 24, 340 (1967); E. Bucher, F. Heiniger, J. Muller, and P. Spitzli, Phys. Lett. 19, 263 (1965).

[2]N. M. Wolcott and R. L. Falge, Jr., Phys. Rev. 171, 591 (1968); N. M. Wolcott, R. L. Falge, L. H. Bennett, and R. E. Watson, Phys. Rev. Lett. 21, 546 (1968); A. Herr and R. Kuentzler, Phys. Status Solidi B 45, *K*1 (1971); R. Kuentzler and R. Jesser, Solid State Commun. 13, 915 (1973).

[3]See, e.g., K. Schubert, *Kristallstrukturen 2-Komponentiger Phasen* (Springer, Berlin, 1964), p. 219.

[4]D. P. Shoemaker, R. E. Marsh, F. J. Ewing, and L. Pauling, Acta Crystallogr. 5, 637 (1952).

[5]W. B. Pearson, *Handbook of Lattice Spacings and Structures of Metals and Alloys* (Pergamon, New York, 1967), Vol. 2.

[6]R. Troć, W. Trzebiatowski, and K. Piprek, Bull. Acad. Pol. Sci. Ser. Sci. Chim. 19, 427 (1971).

[7]*Constitution of Binary Alloys*, edited by M. Hansen (McGraw-Hill, New York, 1958), Vol. 1, *Constitution of Binary Alloys*, edited by R. P. Elliot (McGraw-Hill, New York, 1965), Suppl. 1; *Constitution of Binary Alloys*, edited by F. A. Shunk (McGraw-Hill, New York, 1970), Suppl. 2.

[8]F. Borsa and G. Olcese, Phys. Status Solidi A 17, 631 (1973).

[9]N. I. Sax, *Dangerous Properties of Industrial Materials* (Reinhold, New York, 1968); S. Monch, Metall. 23, 238 (1969).

[10]F. J. Morin and J. P. Maita, Phys. Rev. 129, 1115 (1963).

[11]R. M. Bozorth, H. J. Williams, and D. G. Walsh, Phys. Rev. 103, 572 (1956).

[12]S. Domngang and A. Herr, Solid State Commun. 13, 197 (1973).

[13]G. Ahlers, Phys. Rev. 145, 419 (1966); M. E. Gmelin, C. R. Acad. Sci. 259, 3459 (1964).

[14]J. R. Cooper, C. Rizzuto, and G. Olcese, J. Phys. (Paris) 32, C1-1136 (1971).

[15]For a review see, D. K. Wohlleben and B. R. Coles, in *Magnetism*, edited by G. T. Rado and H. Suhl (Academic, New York, 1973), Vol. V.

[16]W. E. Gardner, J. Penfold, T. F. Smith, and I. R. Harris, J. Phys. F 2, 133 (1972).

[17]N. C. Baenziger and R. E. Rundle, Acta Crystallogr. 2, 258 (1949).

[18]E. I. Gladyshevskii, P. I. Kripyakevich, and D. P. Frankevich, Kristallografiya 8, 788 (1963) [Sov. Phys.-Crystallogr. 8, 628 (1963)].

[19]K. R. Lea, M. J. M. Leask, and W. P. Wolf, J. Phys. Chem. Solids 23, 1381 (1962).

[20]E. Bucher, K. Andres, J. P. Maita, A. S. Cooper, and L. D. Longinotti, J. Phys. (Paris) 32, C1-114 (1971).

[21]E. Bucher and J. P. Maita, Solid State Commun. 13, 215 (1973).

[22]A. J. Freeman and R. E. Watson, Phys. Rev. 127, 2058 (1962).

[23]W. Burton Lewis, in *Magnetic Resonance and Related Phenomena*, edited by I. Ursu (Publishing House of the Academy of Soc. Rep. of Romania, 1971), p. 717.

[24]Y. L. Wang and B. R. Cooper, Phys. Rev. 185, 696 (1969).

[25]B. S. Lee, J. Phys. C 6, 2873 (1973).

[26]G. Williams and L. L. Hirst, Phys. Rev. 185, 407 (1969).

[27]E. Bucher, J. P. Maita, and A. S. Cooper, Phys. Rev. B 6, 2709 (1972).

[28]S. A. Al'tshuler, Zh. Eksp. Teor. Fiz. Pis'ma Red. 3, 177 (1966) [JETP Lett. 3, 112 (1966)].

[29]K. Andres and E. Bucher, J. Appl. Phys. 42, 1522 (1971).

[30]K. Andres and E. Bucher, Phys. Rev. Lett. 28, 1652 (1972).

[31]B. Bleaney, J. Appl. Phys. 34, 1024 (1963).

[32]K. Andres and E. Bucher, Phys. Rev. Lett. 22, 600 (1969).

[33]K. Andres and E. Bucher, Phys. Rev. Lett. 24, 1181 (1970).

[34]I. Peschel and P. Fulde, Z. Phys. 259, 145 (1973).

[35]B. R. Cooper, Phys. Lett. 22, 244 (1966).